The Eighteenth International Symposium on Artificial Life and Robotics 2013 (AROB 18th '13),
Daejeon Convention Center, Daejeon, Korea, January 30-February 1, 2013

Control of a dual arm underwater robot

Shinichi Sagara Radzi Bin Ambar Kenichi Imaike
Department of Mechanical and Control Engineering, Kyushu Institute of Technology
Tobata, Kitakyushu 804-8550, Japan
E-mail: sagara@cntl.kyutech.ac.jp

Abstract: Since Underwater Vehicle-Manipulator Systems (UVMS) are expected to make important roles in ocean exploration, many studies about control of single arm UVMSs have been reported. We have also been proposed a resolved acceleration control (RAC) method for a single arm UVMS. In this paper, we propose a RAC method for a dual arm UVMS. Simulation results show the effectiveness of the proposed control method.

Keywords: Underwater Robot, Manipulator, Control

1 Introduction

Underwater robots are expected to be actively involved in various activities such as researches, environment and ecological investigation at locations mainly in the ocean, river and lakes. Many studies on Underwater Vehicle-Manipulator Systems (UVMS) are performed in recent years [1–7]. However there are only a few experimental studies. We have proposed digital Resolved Acceleration Control (RAC) methods for UVMS [8, 9] and the effectiveness of the RAC methods has been demonstrated by experiments using a floating underwater robot with vertical planar 2-link manipulator.

The main objective of this paper is to design a control system for dual arm UVMS. Many of research studies have been focusing on the development of single arm UVMSs. Sakagami et al. have been proposed a simultaneous operation of dual arm underwater robot [10]. However, there is no study on control of dual arm UVMS. In this paper, we propose a RAC method for dual arm UVMS based on Reference [8]. Simulation results show the effectiveness of the proposed control method.

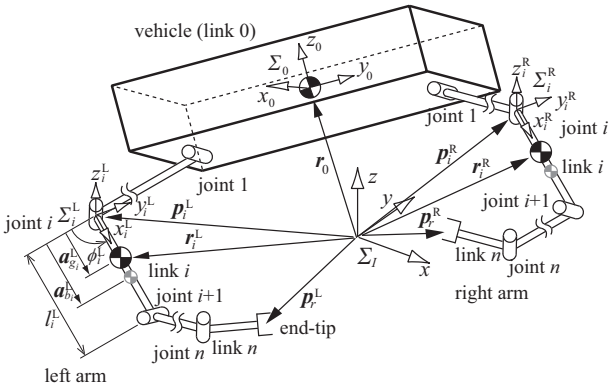

Fig. 1 Model of a dual arm underwater robot

2 Modeling

2.1 UVMS

The underwater robot model used in this paper is shown in Fig. 1. It has a robot base (vehicle) and dual n-DOF manipulators. Thrusters are mounted on the base to provide propulsion for position and attitude control of the base. Symbols used in this paper are defined as follows:

- n^* : number of joint of arm $*$ ($*$=R: Right arm, $*$=L: Left arm)
- Σ_I : inertial coordinate frame
- Σ_0 : base coordinate frame
- Σ_i^* : link i coordinate frame of arm $*$ ($*$=R: Right arm, $*$=L: Left arm)
- ${}^i\boldsymbol{R}_j^*$: coordinate transformation matrix from Σ_j^* to Σ_i^*
- $\boldsymbol{p}_e^*$: position vector of manipulator end-tip with respect to Σ_I
- $\boldsymbol{p}_i^*$: position vector of origin of Σ_i^* with respect to Σ_I
- $\boldsymbol{r}_i^*$: position vector of gravity center of link i^* with respect to Σ_I
- $\boldsymbol{v}_0$: linear velocity vector of origin of Σ_0 with respect to Σ_I
- $\boldsymbol{v}_e^*$: linear velocity vector of manipulator end-tip with respect to Σ_I
- $\boldsymbol{\psi}_0$: roll-pitch-yaw attitude vector of Σ_0 with respect to Σ_I
- $\boldsymbol{\psi}_e^*$: roll-pitch-yaw attitude vector of end-tip of manipulator with respect to Σ_I
- $\boldsymbol{\omega}_i^*$: angular velocity vector of Σ_i^* with respect to Σ_I
- $\boldsymbol{\omega}_e^*$: angular velocity vector of manipulator end-tip with respect to Σ_I
- ϕ_i^* : relative angle of joint i^*
- $\boldsymbol{\phi}$: relative joint angle vector ($= [(\boldsymbol{\phi}^{\mathrm{R}})^T, (\boldsymbol{\phi}^{\mathrm{L}})^T]^T$, and ($\boldsymbol{\phi}^* = [\boldsymbol{\phi}_1^*,\ \boldsymbol{\phi}_2^*,\ \cdots,\ \boldsymbol{\phi}_n^*]^T$)

$\boldsymbol{k}_i^*$: unit vector indicating a rotational axis of joint i^*
m_i^* : mass of link i^*
$\boldsymbol{M}_{a_i}^*$: added mass matrix of link i^* with respect to Σ_i^*
$\boldsymbol{I}_i^*$: inertia tensor of link i^* with respect to Σ_i^*
$\boldsymbol{I}_{a_i}^*$: added inertia tensor of link i^* with respect to Σ_i^*
$\boldsymbol{x}_0$: position and attitude vector of Σ_0 with respect to Σ_I $(= [\boldsymbol{r}_0^T,\ \boldsymbol{\psi}_0^T]^T)$
$\boldsymbol{x}_e^*$: position and attitude vector of $*$ manipulator end-tip with respect to Σ_I $(= [(\boldsymbol{p}_e^*)^T,\ (\boldsymbol{\psi}_e^*)^T]^T)$
$\dot{\boldsymbol{\chi}}_0$: linear and angular vector of Σ_0 with respect to Σ_I $(= [\boldsymbol{v}_0^T,\ \boldsymbol{\omega}_0^T]^T)$
$\dot{\boldsymbol{\chi}}_e^*$: linear and angular vector of $*$ manipulator end-tip with respect to Σ_I $(= [(\boldsymbol{v}_e^*)^T,\ (\boldsymbol{\omega}_e^*)^T]^T)$
$\boldsymbol{a}_{g_i}$: position vector from joint i^* to gravity center of link i^* with respect to Σ_I
$\boldsymbol{a}_{b_i}^*$: position vector from joint i^* to buoyancy center of link i^* with respect to Σ_I
l_i^* : length of link i^*
D_i^* : width of link i^*
V_i^* : volume of link i^*
ρ : fluid density
$C_{d_i}^*$: drag coefficient of link i^*
$\boldsymbol{g}$: gravitational acceleration vector
$\boldsymbol{E}_j$: $j \times j$ unit matrix
$\tilde{\boldsymbol{r}}$: skew-symmetric matrix defined as

$$\tilde{\boldsymbol{r}} = \begin{bmatrix} 0 & -z & y \\ z & 0 & -x \\ -y & x & 0 \end{bmatrix},\ \boldsymbol{r} = \begin{bmatrix} x \\ y \\ z \end{bmatrix}$$

2.2 kinematics

In this subsection, based on the reference [8] kinematic and momentum equations are derived.

First, from Fig. 1 a time derivative of the end-tip position vector $\boldsymbol{p}_e^*$ ($*$ =R: Right arm, L: Left arm) is

$$\boldsymbol{v}_e^* = \boldsymbol{v}_0 + \tilde{\boldsymbol{\omega}}(\boldsymbol{p}_e^* - \boldsymbol{r}_0) + \sum_{i=1}^{n} \{\tilde{\boldsymbol{k}}_i^*(\boldsymbol{p}_e^* - \boldsymbol{p}_i^*)\}\dot{\phi}_i^*. \quad (1)$$

On the other hand, relationship between end-tip angular velocity and joint velocity is expressed with

$$\boldsymbol{\omega}_e^* = \boldsymbol{\omega}_0 + \sum_{i=1}^{n} \boldsymbol{k}_i^* \dot{\phi}_i^*. \quad (2)$$

From Eqs. (1) and (2) the following equation is obtained:

$$\dot{\boldsymbol{\chi}}_e^* = \boldsymbol{A}^* \dot{\boldsymbol{\chi}}_0 + \boldsymbol{B}^* \dot{\boldsymbol{\phi}}^* \quad (3)$$

where

$$\boldsymbol{A}^* = \begin{bmatrix} \boldsymbol{E}_3 & -(\tilde{\boldsymbol{p}}_r^* - \tilde{\boldsymbol{p}}_0) \\ \boldsymbol{0}^* & \boldsymbol{E}_3 \end{bmatrix}, \quad \boldsymbol{B}^* = \begin{bmatrix} \boldsymbol{b}_1^* & \boldsymbol{b}_2^* & \cdots & \boldsymbol{b}_n^* \end{bmatrix}$$

and $\boldsymbol{b}_i^* = [\{\tilde{\boldsymbol{k}}_i^*(\boldsymbol{p}_r^* - \boldsymbol{p}_i^*)\}^T,\ (\boldsymbol{k}_i^*)^T]^T$.

Next, let $\boldsymbol{\eta}$ and $\boldsymbol{\mu}$ be a linear and an angular momentum of the robot including hydrodynamic added mass tensor $\boldsymbol{M}_{a_i}^*$ and added inertia tensor $\boldsymbol{I}_{a_i}^*$ of link i^*. Then

$$\boldsymbol{\eta} = \boldsymbol{M}_{T_0}\dot{\boldsymbol{r}}_0 + \boldsymbol{\eta}^{\mathrm{R}} + \boldsymbol{\eta}^{\mathrm{L}}, \quad (4)$$

$$\boldsymbol{\mu} = \boldsymbol{I}_{T_0}\boldsymbol{\omega}_0 + \tilde{\boldsymbol{r}}_0\boldsymbol{M}_{T_0}\dot{\boldsymbol{r}}_0 + + \boldsymbol{\mu}^{\mathrm{R}} + \boldsymbol{\mu}^{\mathrm{L}} \quad (5)$$

where

$$\boldsymbol{\eta}^* = \sum_{i=1}^{n^*} \boldsymbol{M}_{T_i}^* \dot{\boldsymbol{r}}_i^*, \quad \boldsymbol{\mu}^* = \sum_{i=1}^{n^*} \boldsymbol{I}_{T_i}^* \boldsymbol{\omega}_i^* + \tilde{\boldsymbol{r}}_i^* \boldsymbol{M}_{T_i}^* \dot{\boldsymbol{r}}_i^*$$

and $\boldsymbol{M}_{T_i}^* = m_i^* \boldsymbol{E}_3 + {}^I\boldsymbol{R}_i^* \boldsymbol{M}_{a_i}^* {}^i\boldsymbol{R}_I^*$ and $\boldsymbol{I}_{T_i}^* = {}^I\boldsymbol{R}_i^*(\boldsymbol{I}_i^* + \boldsymbol{I}_{a_i}^*){}^i\boldsymbol{R}_I^*$. Here, linear and angular velocities of gravity center of link i^* are described as

$$\dot{\boldsymbol{r}}_i^* = \boldsymbol{v}_0 + \tilde{\boldsymbol{\omega}}_0(\boldsymbol{r}_i^* - \boldsymbol{r}_0) + \boldsymbol{J}_{v_i}^* \dot{\boldsymbol{\phi}}^*, \quad (6)$$

$$\boldsymbol{\omega}_i^* = \boldsymbol{\omega}_0 + \boldsymbol{J}_{\omega_i}^* \dot{\boldsymbol{\phi}}^*, \quad (7)$$

$$\boldsymbol{J}_{v_i}^* = \begin{bmatrix} \boldsymbol{j}_{i_1}^* & \boldsymbol{j}_{i_2}^* & \cdots & \boldsymbol{j}_{i_i}^* & \boldsymbol{0} & \cdots & \boldsymbol{0} \end{bmatrix},$$
$$\boldsymbol{J}_{\omega_i}^* = \begin{bmatrix} \boldsymbol{k}_1^* & \boldsymbol{k}_2^* & \cdots & \boldsymbol{k}_i^* & \boldsymbol{0} & \cdots & \boldsymbol{0} \end{bmatrix}$$

where $\boldsymbol{j}_{i_j}^* = \boldsymbol{k}_j^* \times (\boldsymbol{r}_i^* - \boldsymbol{p}_j^*)$. Therefore, the following equation is obtained from Eqs. (4)-(7):

$$\boldsymbol{s} = [\boldsymbol{\eta}^T,\ \boldsymbol{\mu}^T]^T = \boldsymbol{C}\dot{\boldsymbol{\chi}}_0 + \boldsymbol{D}\dot{\boldsymbol{\phi}} \quad (8)$$

where

$$\boldsymbol{C} = \begin{bmatrix} \boldsymbol{c}_{11} & \boldsymbol{c}_{12} \\ \boldsymbol{c}_{21} & \boldsymbol{c}_{22} \end{bmatrix},$$

$$\boldsymbol{D} = \begin{bmatrix} \boldsymbol{d}_{11}^{\mathrm{R}} & \boldsymbol{d}_{12}^{\mathrm{R}} & \cdots & \boldsymbol{d}_{1n^{\mathrm{R}}}^{\mathrm{R}} & \boldsymbol{d}_{11}^{\mathrm{L}} & \boldsymbol{d}_{12}^{\mathrm{L}} & \cdots & \boldsymbol{d}_{1n^{\mathrm{L}}}^{\mathrm{L}} \\ \boldsymbol{d}_{21}^{\mathrm{R}} & \boldsymbol{d}_{22}^{\mathrm{R}} & \cdots & \boldsymbol{d}_{2n^{\mathrm{R}}}^{\mathrm{R}} & \boldsymbol{d}_{21}^{\mathrm{L}} & \boldsymbol{d}_{22}^{\mathrm{L}} & \cdots & \boldsymbol{d}_{2n^{\mathrm{L}}}^{\mathrm{L}} \end{bmatrix},$$

$$\boldsymbol{c}_{11} = \boldsymbol{M}_{T_0} + \sum_{i=1}^{n^{\mathrm{R}}} \boldsymbol{M}_{T_i}^{\mathrm{R}} + \sum_{i=1}^{n^{\mathrm{L}}} \boldsymbol{M}_{T_i}^{\mathrm{L}},$$

$$\boldsymbol{c}_{12} = -\sum_{i=1}^{n^{\mathrm{R}}} \boldsymbol{M}_{T_i}^{\mathrm{R}}(\tilde{\boldsymbol{r}}_i^{\mathrm{R}} - \tilde{\boldsymbol{r}}_0) - \sum_{i=1}^{n^{\mathrm{L}}} \boldsymbol{M}_{T_i}^{\mathrm{L}}(\tilde{\boldsymbol{r}}_i^{\mathrm{L}} - \tilde{\boldsymbol{r}}_0),$$

$$\boldsymbol{c}_{21} = \tilde{\boldsymbol{r}}_0\boldsymbol{M}_{T_0} + \sum_{i=1}^{n^{\mathrm{R}}} \tilde{\boldsymbol{r}}_i^{\mathrm{R}} \boldsymbol{M}_{T_i}^{\mathrm{R}} + \sum_{i=1}^{n^{\mathrm{L}}} \tilde{\boldsymbol{r}}_i^{\mathrm{L}} \boldsymbol{M}_{T_i}^{\mathrm{L}},$$

$$\boldsymbol{c}_{22} = \boldsymbol{I}_{T_0} + \sum_{i=1}^{n^{\mathrm{R}}} \boldsymbol{I}_{T_i}^{\mathrm{R}} - \sum_{i=1}^{n^{\mathrm{R}}} \tilde{\boldsymbol{r}}_i^{\mathrm{R}} \boldsymbol{M}_{T_i}^{\mathrm{R}}(\tilde{\boldsymbol{r}}_i^{\mathrm{R}} - \tilde{\boldsymbol{r}}_0)$$
$$+ \sum_{i=1}^{n^{\mathrm{L}}} \boldsymbol{I}_{T_i}^{\mathrm{L}} - \sum_{i=1}^{n^{\mathrm{L}}} \tilde{\boldsymbol{r}}_i^{\mathrm{L}} \boldsymbol{M}_{T_i}^{\mathrm{L}}(\tilde{\boldsymbol{r}}_i^{\mathrm{L}} - \tilde{\boldsymbol{r}}_0),$$

$$\boldsymbol{d}_{1i}^* = \sum_{j=i}^{n^*} \boldsymbol{M}_{T_i}^* \tilde{\boldsymbol{k}}_i^*(\boldsymbol{r}_j^* - \boldsymbol{p}_i^*),$$

$$\boldsymbol{d}_{2i}^* = \sum_{j=i}^{n^*} \boldsymbol{I}_{T_j}^* \boldsymbol{k}_i^* + \tilde{\boldsymbol{r}}_j^* \boldsymbol{M}_{T_j}^* \tilde{\boldsymbol{k}}_i^*(\boldsymbol{r}_j^* - \boldsymbol{p}_i^*).$$

Here, we assume that the added mass and added inertia are constant. In reality, the added mass and inertia are variable but the influence of the variation is compensated by a control method in section 3.

2.3 Equation of motion

Considering the hydrodynamic forces described above and using the Newton-Euler formulation, the following equation of motion can be obtained:

$$\boldsymbol{M}(\boldsymbol{q}_1)\ddot{\boldsymbol{q}}_2 + \boldsymbol{b}_C(\boldsymbol{q}_1,\ \dot{\boldsymbol{q}}_2) + \boldsymbol{f}_D = \boldsymbol{u} \tag{9}$$

where $\boldsymbol{q}_1 = [\boldsymbol{x}_0^T,\ \boldsymbol{\phi}^T]^T$ and $\dot{\boldsymbol{q}}_2 = [\dot{\boldsymbol{\chi}}_0^T,\ \dot{\boldsymbol{\phi}}^T]^T$, $\boldsymbol{M}$ is the inertia matrix including the added mass $\boldsymbol{M}_{a_i}^*$ and inertia $\boldsymbol{I}_{a_i}^*$, $\boldsymbol{b}_C$ is the vector of Coliolis and centrifugal forces, $\boldsymbol{f}_D$ is the vector consisting of the drag, gravitational and buoyant forces and moments, $\boldsymbol{u} = [\boldsymbol{f}_0^T,\ \boldsymbol{\tau}_0^T, \boldsymbol{\tau}_m^T]^T$, $\boldsymbol{f}_0$ and $\boldsymbol{\tau}_0$ are the force and torque vectors of vehicle, $\boldsymbol{\tau}_m$ is the joint torque vector of manipulator. Furthermore, the relationship between $\boldsymbol{\omega}_*$ and $\dot{\boldsymbol{\psi}}_\dagger = [\psi_{r_\dagger},\ \psi_{p_\dagger},\ \psi_{y_\dagger}]^T$ ($\dagger = 0,\ e_\mathrm{R},\ e_\mathrm{L}$) is described as

$$\boldsymbol{\omega}_\dagger = \boldsymbol{S}_{\boldsymbol{\psi}_\dagger}\dot{\boldsymbol{\psi}}_\dagger \tag{10}$$

where

$$\boldsymbol{S}_{\boldsymbol{\psi}_\dagger} = \begin{bmatrix} \cos\psi_{p_\dagger}\cos\psi_{y_\dagger} & -\sin\psi_{y_\dagger} & 0 \\ \cos\psi_{p_\dagger}\sin\psi_{y_\dagger} & \cos\psi_{y_\dagger} & 0 \\ \sin\psi_{p_\dagger} & 0 & 1 \end{bmatrix}.$$

Thus the relationship between $\dot{\boldsymbol{q}}_1$ and $\dot{\boldsymbol{q}}_2$ is described as

$$\dot{\boldsymbol{q}}_2 = \boldsymbol{S}\dot{\boldsymbol{q}}_1 \tag{11}$$

where $\boldsymbol{S} = \mathrm{bolckdiag}\left\{\boldsymbol{E}_3, \boldsymbol{S}_{\boldsymbol{\psi}_0}, \boldsymbol{E}_{(n^\mathrm{R}+n^\mathrm{R})}\right\}$.

3 Digital RAC [8]

Differentiating Eqs. (3) and (8) with respect to time, the following equation can be obtained:

$$\boldsymbol{W}(t)\boldsymbol{\alpha}(t) = \beta(t) + \boldsymbol{f}(t) - \dot{\boldsymbol{W}}(t)\boldsymbol{v}(t) \tag{12}$$

where

$$\boldsymbol{W} = \begin{bmatrix} \boldsymbol{C}+\boldsymbol{E_6} & \boldsymbol{D} \\ \boldsymbol{A} & \boldsymbol{B} \end{bmatrix},\ \boldsymbol{\alpha} = \begin{bmatrix} \ddot{\boldsymbol{\chi}}_0 \\ \ddot{\boldsymbol{\phi}} \end{bmatrix}, \beta = \begin{bmatrix} \ddot{\boldsymbol{\chi}}_0 \\ \ddot{\boldsymbol{\chi}}_e \end{bmatrix},$$

$$\boldsymbol{f} = \begin{bmatrix} \dot{\boldsymbol{s}} \\ \boldsymbol{0} \end{bmatrix},\ \boldsymbol{v} = \begin{bmatrix} \dot{\boldsymbol{\chi}}_0 \\ \dot{\boldsymbol{\phi}} \end{bmatrix},\ \ddot{\boldsymbol{\chi}}_e = \begin{bmatrix} \ddot{\boldsymbol{\chi}}_e^\mathrm{R} \\ \ddot{\boldsymbol{\chi}}_e^\mathrm{L} \end{bmatrix},$$

$$\boldsymbol{A} = \mathrm{blockdiag}\{\boldsymbol{A}^\mathrm{R}, \boldsymbol{A}^\mathrm{L}\},\ \boldsymbol{B} = \mathrm{blockdiag}\{\boldsymbol{B}^\mathrm{R}, \boldsymbol{B}^\mathrm{L}\}$$

and $\dot{\boldsymbol{s}}$ is the external force including hydrodynamic force and thrust of the thruster which act on the base.

Discretizing Eq. (12) by a sampling period T, and applying $\boldsymbol{\beta}(k)$ and $\dot{\boldsymbol{W}}(k)$ to the backward Euler approximation, the following equation can be obtained:

$$\begin{aligned} T\boldsymbol{W}(k)\boldsymbol{\alpha}(k-1) = {} & \boldsymbol{\nu}(k) - \boldsymbol{\nu}(k-1) + T\boldsymbol{f}(k) \\ & - \{\boldsymbol{W}(k) - \boldsymbol{W}(k-1)\}\boldsymbol{v}(k) \end{aligned} \tag{13}$$

where $\boldsymbol{\nu} = \left[\dot{\boldsymbol{\chi}}_0^T,\ \dot{\boldsymbol{\chi}}_e^T\right]^T$. Note that computational time delay is introduced to Eq. (13), and the discrete time kT is abbreviated to k.

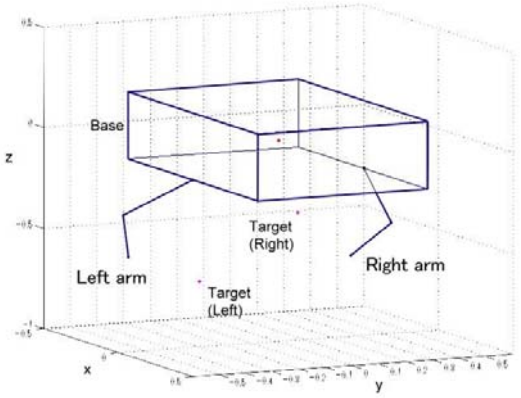

Fig. 2 Simulation model

Table 1 Physical parameters

	Base	Link 1	Link 2
Mass [kg]	23.25	4.65	3.1
Moment of inertia [kgm^2]	2.40	0.075	0.075
Link length [m]	0.5	0.3	0.3
Drag coefficient	1.2	1.0	1.0

For Eq. (13) the desired acceleration is defined as follows:

$$\begin{aligned} \boldsymbol{\alpha}_d(k) = {} & \frac{1}{T}\boldsymbol{W}^\sharp(k)\left[\boldsymbol{\nu}_d(k+1) - \boldsymbol{\nu}_d(k)\right. \\ & \left. + \boldsymbol{\Lambda}\boldsymbol{e}_\nu(k) + T\boldsymbol{f}(k)\right] \end{aligned} \tag{14}$$

$$\boldsymbol{\nu}_d(k) = \frac{\boldsymbol{S}_{0e}}{T}\left\{\boldsymbol{x}_d(k) - \boldsymbol{x}_d(k-1) + \boldsymbol{\Gamma}\boldsymbol{e}_x(k-1)\right\} \tag{15}$$

where $\boldsymbol{e}_\nu(k) = \boldsymbol{\nu}_d(k) - \boldsymbol{\nu}(k)$, $\boldsymbol{e}_x(k) = \boldsymbol{x}_d(k) - bmx(k)$, $\boldsymbol{S}_{0e} = \mathrm{blockdiag}\{\boldsymbol{E}_3, \boldsymbol{S}_{\psi 0}, \boldsymbol{E}_3, \boldsymbol{S}_{\psi e_\mathrm{R}}, \boldsymbol{E}_3, \boldsymbol{S}_{\psi e_\mathrm{L}}\}$, and $W^\sharp$ is the pseudoinverse of W, $\boldsymbol{x}_d$ is the desired value of $\boldsymbol{x} = [\boldsymbol{x}_0^T, \left(\boldsymbol{x}_0^\mathrm{R}\right)^T, \left(\boldsymbol{x}_0^\mathrm{L}\right)^T]^T$, $\boldsymbol{\Lambda} = \mathrm{diag}\{\lambda_i\}$ and $\boldsymbol{\Gamma} = \mathrm{diag}\{\gamma_i\}$ (i =1, $\cdots$, $(6 + n^\mathrm{R} + n^\mathrm{L})$) are the velocity and the position feedback gain matrices.

From Eqs. (13), (14) and (15), if λ_i and γ_i are selected to satisfy $0 < \lambda_i < 1$ and $0 < \gamma_i < 1$, respectively, and the convergence of the acceleration error, $\boldsymbol{e}_\alpha(k) = \boldsymbol{\alpha}_d(k) - \boldsymbol{\alpha}(k)$, tends to zero as k tends to infinity, then the convergence of $\boldsymbol{e}_\nu(k)$ and $\boldsymbol{e}_x(k)$ to zero as k tends to infinity can be ensured.

4 Simulation

In this section, simulations using a robot shown in Fig. 2 are done. Physical parameters of the robot are shown in Table 1. These parameters are based on the Reference [8].

The simulation was carried out under the following condition.

The initial relative angles of the robot were $\phi_1^{\mathrm{R}} = -\pi/9$[rad], $\phi_2^{\mathrm{R}} = \pi/9$[rad], $\phi_1^{\mathrm{L}} = \pi/3$[rad] and $\phi_2^{\mathrm{L}} = -\pi/9$[rad]. The desired end-tip positions were set up along a straight path from the initial positions to the targets in $y - z$ plane. calculated from trapezoidal velocity pattern. On the other hand, the basic desired position and attitude of vehicle were set up the initial values. The sampling period was T=1/60[s] and the feedback gains were $\boldsymbol{\Lambda} = \boldsymbol{\Gamma}$ = diag { 0.01, 0.01, 0.01, 0.01, 0.01, 0.01, 0, 0.2, 0.2, 0, 0, 0, 0, 0.2, 0.2, 0, 0, 0 }.

The simulation result is shown in Fig. 3. In this figure, (a) is the motion of the robot, (b) is the time history. From Fig. 3 it can be seen that the end-tips of two armsr and base follow the reference trajectories in spite of the influence of the hydrodynamic forces and the tracking errors are very small. The experimental result shows that the control performance can be improved by using the proposed method.

5 Conclusion

In this paper, we propose a RAC method for dual arm UVMS based on Reference [8]. Simulation results showed the effectiveness of the proposed control method.

References

[1] H. Maheshi *et al.*, "A Coordinated Control of an Underwater Vehicle and Robotic Manipulator", *J. Robotic Systems*, Vol. 8, No. 3, pp. 339 – 370, 1991.

[2] T. W. McLain *et al.*, "Experiments in the Coordinated Control of an Underwater Arm/Vehicle System", *Autonomous Robots 3*, Kluwer Academic Publishers, pp. 213 – 232, 1996.

[3] G. Antonelli *et al.*, "Tracking Control for Underwater Vehicle-Manipulator Systems with Velocity Estimation", *IEEE J. Oceanic Eng.*, Vol. 25, No. 3, pp. 399 – 413, 2000.

[4] N. Sarkar and T. K. Podder, "Coordinated Motion Planning and Control of Autonomous Underwater Vehicle-Manipulator Systems Subject to Drag Optimization", *IEEE J. Oceanic Eng.*, Vol. 26, No. 2, pp. 228 – 239, 2001.

[5] G. Antonelli, *Underwater Robotics*, Springer, pp. 1194–1206, 2003.

[6] B. Xu, S. R. Pandian, N. Sakagami and F. Petry, "Neuro-Fuzzy Control of Underwater Vehicle-Manipulator Systems", *J. Franklin Institute*, 349, pp. 1125–1138, 2012.

[7] S. Mohan and J. Kim, "Indirect Adaptive Control of an Autonomous Underwater Vehicle-Manipulator System for Underwater Manipulation Tasks", Ocean Engineering, Vol. 54, pp. 233–243, 2012.

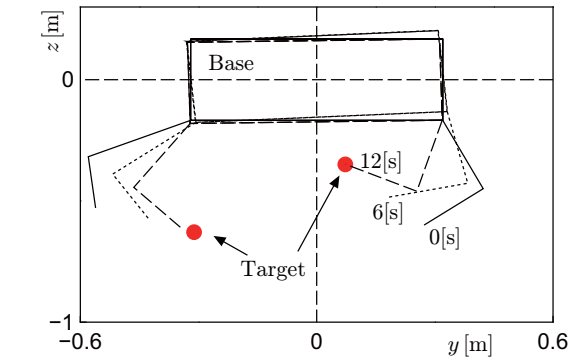

(a) motion

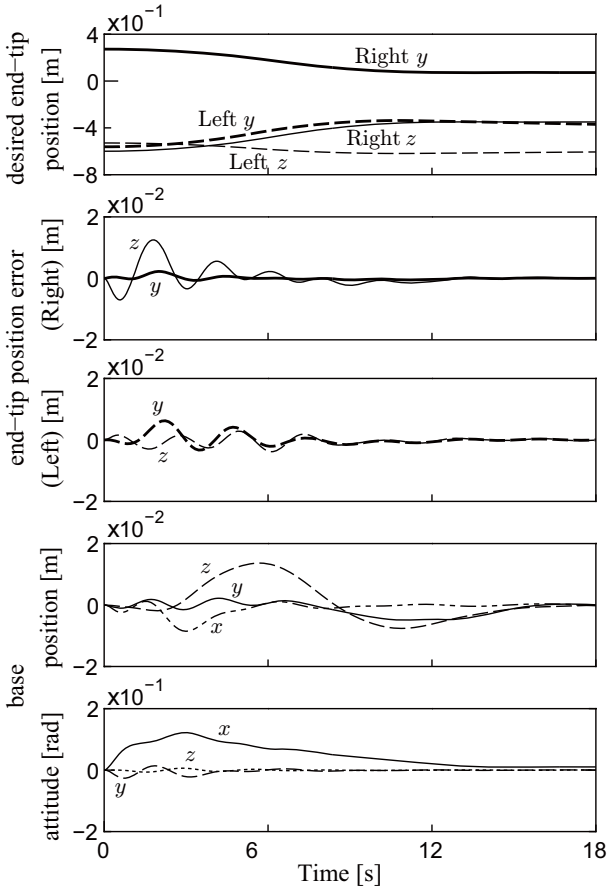

(b) time history

Fig. 3 Simulation result

[8] S. Sagara *et al.*,"Digital RAC for Underwater Vehicle-Manipulator Systems Considering Singular Configuration", *J. Artificial Life and Robotics*, Vol. 10, No. 2, pp. 106 – 111, 2006.

[9] S. Sagara *et al.*,"Digital RAC with a Disturbance Observer for Underwater Vehicle-Manipulator Systems", *J. Artificial Life and Robotics*, Vol. 15, No. 3, pp. 270 – 274, 2010.

[10] N. Sakagami *et al.*, "Development of a Human-Sized ROV with Dual-Arm", Proc. MTS/IEEE OCEANS 2010, 2010.